PERGAMON

International Journal of Heat and Mass Transfer 41 (1998) 3397–3408

International Journal of HEAT and MASS TRANSFER

Unsteady free convection flow in the stagnation-point region of a three-dimensional body

A. Slaouti[a,*], H. S. Takhar[a,†], G. Nath[b]

[a] *Department of Mechanical Engineering, Manchester Metropolitan University, Manchester M1 5GD, U.K.*
[b] *Department of Mathematics, Indian Institute of Science, Bangalore, 560072, India*

Received 9 October 1997; in final form 4 February 1998

Abstract

The unsteady free convection flow in the stagnation-point region of a heated three-dimensional body placed in an ambient fluid is studied under boundary layer approximations. We have considered the case where there is an initial steady state that is perturbed by a step-change in the wall temperature. The non-linear coupled partial differential equations governing the free convection flow are solved numerically using a finite difference scheme. The presented results show the temporal development of the momentum and thermal boundary layer characteristics.

Nomenclature

a, b principal curvatures of the body at the stagnation point
c curvature ratio at the stagnation point
C_{fx} surface skin friction coefficient in the x direction
C_{fy} surface skin friction coefficient in the y direction
F dimensionless velocity component in the x direction
g acceleration due to gravity
G dimensionless temperature
Gr Grashof number
Nu Nusselt number
Pr Prandtl number
S dimensionless velocity component in the y direction
t time
t^* dimensionless transformed independent variable based on time
T temperature
u, v, w velocity components in the x, y and z directions, respectively
x, y, z local orthogonal coordinates with x and y axes along the body surface and z axis normal to the surface.

Greek symbols
α thermal diffusivity
β bulk coefficient of thermal expansion
ε dimensionless constant
η dimensionless transformed independent variable based on z
μ fluid dynamic viscosity
ν fluid kinematic viscosity
ρ fluid density.

Subscripts
i initial condition
o condition at time $t = 0$
t denotes partial derivative with respect to t
t* denotes partial derivative with respect to t^*
w wall condition
x denotes partial derivative with respect to x
y denotes partial derivative with respect to y
z denotes partial derivative with respect to z
∞ condition in the ambient fluid.

Superscript
′ denotes derivative with respect to η.

1. Introduction

Free convection phenomena arise in nature and in industries when a heated surface or substance is brought

* Corresponding author.
† Also at the Manchester School of Engineering, University of Manchester, Manchester M13 9PL, U.K.

0017–9310/98 $19.00
PII: S0017–9310(98)00080–5

into contact with a mass of fluid. The temperature changes cause density variations leading to buoyancy forces. This process of heat transfer is encountered in atmospheric and oceanic circulations, in the handling of spent nuclear reactor fuel assemblies, in the design of solar energy collectors, in the process of frost formation involving low temperature surfaces etc. There is a great deal of information available about the steady free convection boundary layer flow over bodies of various shapes. Critical reviews of the relevant literature are given by Ede [1], Gebhart [2] and Gebhart et al. [3]. The steady free convection boundary layer flow over three-dimensional bodies has been studied by several investigators ([4]–[10]). The analogous unsteady case has attracted little attention in the literature.

In free convection flows the driving mechanism is the surface temperature or surface heat flux. Hence, when the surface of a body is under transient heating, the surface temperature is a function of time and gives rise to transient free convection flows. An analysis of the transient free convection problems is important since these have wide applications in nuclear reactor technology, floated gyrocompasses and liquid heat sink cooling of re-entry vehicles. The motivation for studying transient free convection flows in the stagnation-point region is due to the fact that the heat transfer is maximum at the stagnation point and unsteadiness in the flow field can be caused either by a sudden change in the wall temperature or by a time-dependent wall temperature. It may be remarked that even though the stagnation-point solutions are valid in a small region in the vicinity of the stagnation point of a three-dimensional body, they represent several physical flows of engineering significance. The stagnation-point solutions may also serve as a starting solution for the solution over the entire body. The governing equations for the stagnation-point flow can be reduced to a system of partial differential equations involving only two independent variables, whereas the solution over the entire three-dimensional body would involve four independent variables. The unsteadiness in the flow field increases the dimension of the problem by one and thus increases the complexity of the problem. Also, the boundary layer thickness grows with time and the solution may blow up after a finite time. This aspect has been discussed by Wilks and Hunt [11] for boundary layer equations for natural convection flow and by Childress et al. [12] for two-dimensional Euler and Navier–Stokes equations.

Although the transient free convection flow over three-dimensional bodies has not been studied very much, the corresponding two-dimensional case (mostly involving flat plates) has been investigated by a number of workers. Hellums and Churchill [13] presented a numerical solution of the coupled time-dependent boundary layer equations governing transient natural convection over a semi-infinite vertical plate in air. Goldstein and Briggs [14] and Nanbu [15] studied the same problem analytically. The critical time for the end of pure conduction obtained by Hellums and Churchill [13] was found to be about 15 per cent lower than that of Goldstein and Briggs [14] and Nanbu [15]. Elliot [16] analysed the problem of unsteady free convection boundary layer flow over two-dimensional and axisymmetric bodies for a step input in the surface temperature. Miyamoto [17] studied the effect of variable fluid properties on the transient and steady-state free convection flows. Carey [18] investigated the transient natural convection flow at high Prandtl number using the method of matched asymptotic expansions. Soundalgekar and Ganesan [19] considered the effect of mass transfer on transient free convection flow on a vertical plate with constant heat flux. Williams et al. [20] studied the unsteady free convection flow over a vertical flat plate under the assumption that the wall temperature varies with time and distance and found possible semi-similar solutions for a variety of classes of wall temperature distributions. Singh and Soundalgekar [21] considered transient free convection flow of cold water over a vertical porous plate. Sattar and Alam [22] investigated the unsteady free convection flow of a viscous, incompressible and electrically conducting fluid past a moving infinite vertical porous plate taking into account the thermal diffusion effect. The unsteadiness in the flow field was introduced by the time-dependent velocity of the moving plate. Li [23] examined the effect of the magnetic field on low-frequency oscillating natural convection flow on a vertical plate. Kumari et al. [24] studied the transient free convection flow over a continuous moving vertical sheet in an ambient fluid. The unsteadiness in the flow field was caused by the time-dependent velocity of the sheet. Both constant temperature and constant heat flux conditions were considered. Kumari and Nath [25] considered the unsteady free convection flow in the stagnation-point region of a heated porous three-dimensional body where the unsteadiness in the flow field was caused by a time-dependent wall temperature. The semi-similar equations governing the flow were solved numerically using an implicit finite-difference scheme. The heat transfer was found to be strongly dependent on time, whereas the skin friction was weakly dependent on it. The increase in the Prandtl number resulted in an increase in heat transfer but in a decrease of the skin friction. The mass transfer was found to affect both the heat transfer and skin friction significantly.

In this paper, the unsteady convection flow of an incompressible viscous fluid in the stagnation-point region of a heated three-dimensional body is considered. We have considered the situation in which there is an initial steady state that is perturbed by a step-change in the wall temperature. The non-linear coupled partial differential equations governing the flow are solved numerically using a finite-difference scheme developed by Nakamura [26]. The time-dependent development of the

boundary layer is computed until a new steady state is reached. The initial steady state results are compared with those of Poots [4] and of Banks [8].

2. Problem formulation

We consider the unsteady laminar free convection flow of an incompressible viscous fluid in the stagnation-point region of a heated three-dimensional body placed in an ambient fluid. All fluid properties are assumed to be constant except for the density changes which give rise to buoyancy forces in the momentum equations. These buoyancy forces cause fluid motion. It is assumed that the temperature of the ambient fluid is constant and that viscous dissipation terms are negligible in the stagnation-point region. We investigate the situation for which an initial steady state is perturbed by a step-change in the wall temperature. A locally orthogonal set of coordinates (x, y, z) is chosen with the origin O at the lowest stagnation point, with x and y the coordinates along the body surface and z the coordinate perpendicular to the body surface at O (see Fig. 1). Gravity g is normal to the surface at $x = 0$ and $y = 0$ and acts opposite to the z direction. Let u, v and w denote the velocity components along the x, y and z directions, respectively. The parameters a and b are the curvatures of the body measured in the planes $y = 0$ and $x = 0$, respectively, and because of the choice of axes, a and b are the principal curvatures at O. The parameter $c = b/a$ represents the nature of the three-dimensional stagnation point. Here a and b are assumed to be positive so that solutions of the resulting equations lead to stagnation points which are nodal points of attachment $(0 \leqslant c \leqslant 1)$. However, a or b could also be negative which leads to saddle points of attachment $(-1 \leqslant c \leqslant 0)$. Since most shapes of practical interest lie between cylinder $(c = 0)$ and sphere $(c = 1)$ we have confined our analysis to nodal points of attachment only $(0 \leqslant c \leqslant 1)$. At the lowest stagnation point the direction of gravity g is perpendicular to x and y directions, but in the vicinity of the lowest stagnation point g is inclined to both directions. This gives rise to buoyancy induced pressure gradients in x and y directions, but they are very small compared to the buoyancy forces in those directions [27]. Hence, in the vicinity of the lowest stagnation point O, the components of the buoyancy force in x, y and z directions are [7]:

$$\rho g\beta ax(T-T_\infty), \rho g\beta by(T-T_\infty), 0.$$

Under the above assumptions, the boundary layer equations of continuity, motion and energy governing the unsteady free convection flow are given by:

$$u_x + v_y + w_z = 0 \tag{1}$$

$$u_t + uu_x + vu_y + wu_z - g\beta ax(T-T_\infty) = vu_{zz} \tag{2}$$

$$v_t + uv_x + vv_y + wv_z - g\beta by(T-T_\infty) = vv_{zz} \tag{3}$$

$$T_t + uT_x + vT_y + wT_z = \alpha T_{zz} \tag{4}$$

The initial conditions are given by:

$$t = 0, x \geqslant 0, y \geqslant 0, z \geqslant 0 : u = u_i, v = v_i, w = w_i, T = T_i \tag{5}$$

The boundary conditions for $t > 0$ are:

$$\begin{aligned} z = 0, x \geqslant 0, y \geqslant 0: &\quad u = v = w = 0, \\ &\quad T = T_w = T_\infty + (T_{wo} - T_\infty)(1+\varepsilon) \\ z \to \infty, x \geqslant 0, y \geqslant 0: &\quad u = v = 0, T = T_\infty \\ x = 0, y \geqslant 0, z > 0: &\quad u = v = 0, T = T_\infty \\ y = 0, x \geqslant 0, z > 0: &\quad u = v = 0, T = T_\infty. \end{aligned} \tag{6}$$

The system of partial differential equations (1)–(4) con-

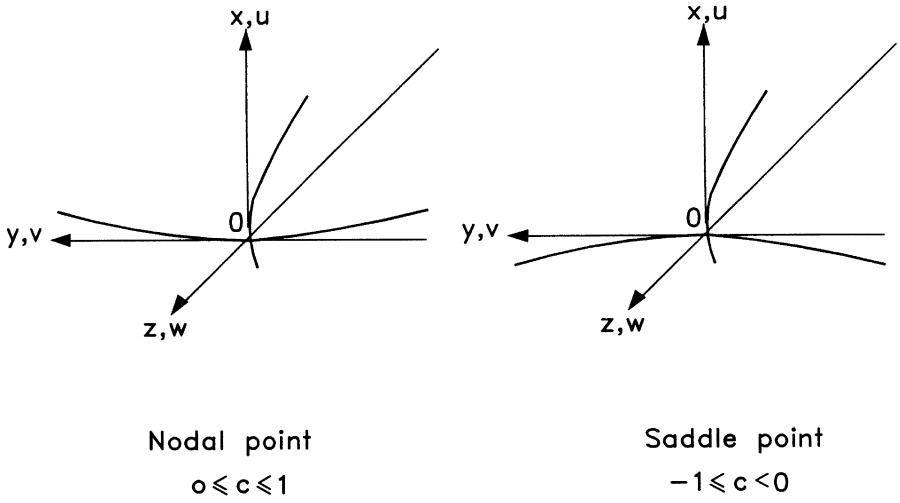

Fig. 1. Schematic representation of coordinates and velocity components

taining four independent variables t, x, y, z can be reduced to a system of semi-similar equations with two independent variables η and t^* by using the following transformations:

$$\eta = (Gr)^{1/4} az, \quad Gr = g\beta(T_{wo} - T_\infty)/(a^3 v^2),$$

$$t^* = va^2 (Gr)^{1/2} t$$

$$f' = F, \quad s' = S, \quad u = va^2 x (Gr)^{1/2} F(\eta, t^*)$$

$$v = va^2 cy (Gr)^{1/2} S(\eta, t^*), \quad w = -va(Gr)^{1/4}(f + cs)$$

$$T - T_\infty = (T_{wo} - T_\infty) G(\eta, t^*), \quad Pr = v/\alpha. \tag{7}$$

Consequently, equation (1) is identically satisfied and equations (2)–(4) reduce to:

$$F'' + (f + cs)F' - F^2 + G - F_{t^*} = 0 \tag{8}$$

$$S'' + (f + cs)S' - cS^2 + cG - S_{t^*} = 0 \tag{9}$$

$$Pr^{-1} G'' + (f + cs)G' - G_{t^*} = 0 \tag{10}$$

and the boundary conditions are expressed as

$$F = S = 0, G = 1 + \varepsilon \quad \text{at } \eta = 0$$

$$F = S = G = 0 \quad \text{as } \eta \to \infty. \tag{11}$$

Also

$$f = \int_0^\eta F \, d\eta, s = \int_0^\eta S \, d\eta. \tag{12}$$

We have assumed that the flow is steady at time $t^* = 0$ and becomes unsteady for $t^* > 0$ due to a step change in the wall temperature. Hence the initial conditions are given by the steady-state equations obtained by putting $t^* = F_{t^*} = S_{t^*} = G_{t^*} = 0$ in equations (8)–(10). These are given by

$$F'' + (f + cs)F' - F^2 + G = 0 \tag{13}$$

$$S'' + (f + cs)S' - cS^2 + cG = 0 \tag{14}$$

$$Pr^{-1} G'' + (f + cs)G' = 0 \tag{15}$$

and the boundary conditions are given by

$$F = S = 0, G = 1 \quad \text{at } \eta = 0$$

$$F = S = G = 0 \quad \text{as } \eta \to \infty. \tag{16}$$

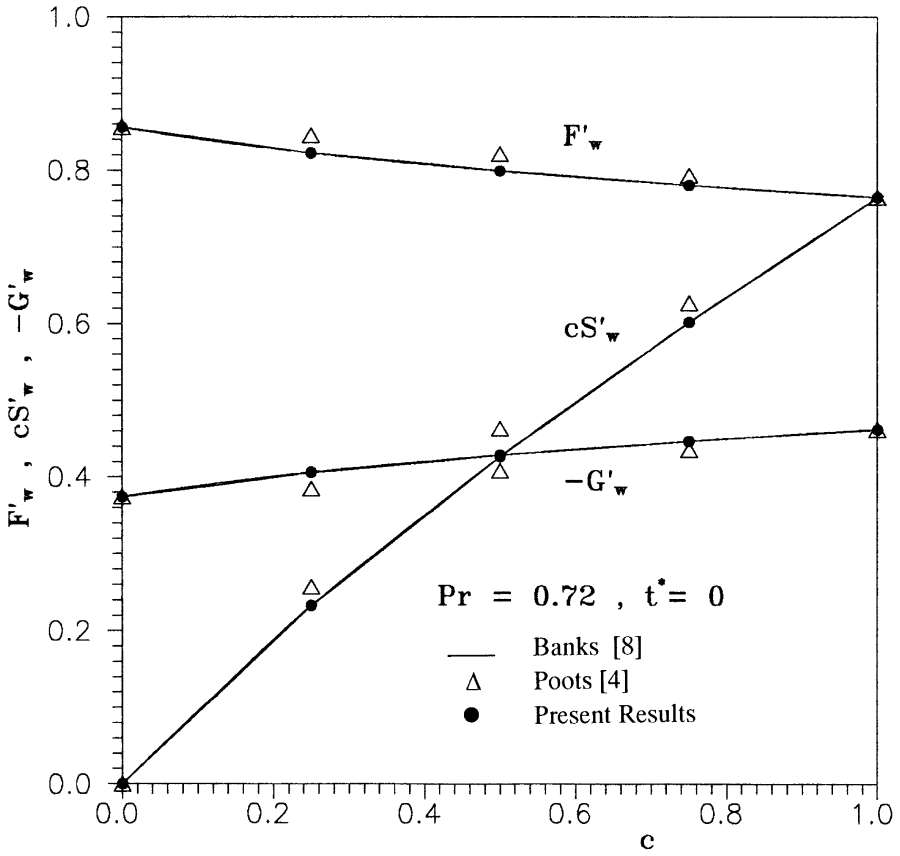

Fig. 2. Comparison of the surface skin friction parameters in the x and y directions (F'_w, cS'_w) and the surface heat transfer parameter ($-G'_w$) at $t^* = 0$ for $Pr = 0.72$

Here η and t^* are the dimensionless transformed independent variables; F and S are the dimensionless velocity components in the x and y directions, respectively; G is the dimensionless temperature; Gr is the Grashof number; Pr is the Prandtl number; prime denotes the derivative with respect to η and the subscript t^* denotes the derivative with respect to t^*.

It may be noted that equations (13)–(15) are essentially the same as those of Poots [4] except for some minor differences due to the slightly different transformations that he used. Also, these equations are identical to those of Banks [8] if we put $cs = \bar{s}$.

The surface skin friction coefficients in the x and y directions (C_{fx}, C_{fy}) and the surface heat transfer coefficient in terms of the Nusselt number (Nu) are given by

$$C_{fx} = \mu(\partial u/\partial z)_w/(\rho v^2 a^3 x) = (Gr)^{3/4} F'_w$$

$$C_{fy} = \mu(\partial v/\partial z)_w/(\rho v^2 a^3 y) = (Gr)^{3/4} cS'_w$$

$$Nu = a^{-1}(\partial T/\partial z)_w/(T_{w0} - T_\infty) = (Gr)^{1/4} G'_w \quad (17)$$

where ρ and μ are the density and dynamic viscosity of the fluid, respectively.

3. Method of solution

Equations (8)–(10) under boundary conditions (11) and initial conditions (13)–(15), are solved numerically using a finite-difference scheme developed by Nakamura, which is described in detail in Ref. [26]. Hence, for the sake of completeness, we present here only an outline of this method. Equation (8)–(10) are coupled non-linear parabolic partial differential equations in F, S and G. The variables f and s in equations (8)–(10) are considered as non-linear coefficients and are evaluated by numerical integration from F and S (see equation (12)). Equations (8)–(10) are discretised using the central difference approximation in the η coordinate and backward difference approximation in the t^* coordinate. For the time step k, the discretised equations for (8)–(10) become tridiagonal equations. This system of equations for each time step requires an iterative procedure due to the presence of non-linear coefficients. Successive substitution and iteration are continued for each time step until convergence is reached. Equations (13)–(15) under boundary conditions (16) were solved by using a double shooting method (Takhar [28]) in order to accurately obtain the initial values of the various functions at time $t^* = 0$.

4. Results and discussion

The governing equations have been solved numerically using the method described earlier. Convergence for the set of equations was reached when all the discretised values of the functions f, s and G converged within a value set at 10^{-6}. The effect of step sizes $\Delta\eta$ and Δt^* on the solutions was carefully investigated. It was found that a step $\Delta\eta$ of 0.10 was adequate as the solutions showed no difference with the smaller values. Along the time t^* coordinate, a step Δt^* of 0.005 was found to be necessary in the initial temporal development of the solutions ($0 < t^* \leqslant 0.10$) whereas a much larger value can be used in the later stages ($t^* > 0.10$) where the variations are much more gradual. For the present results we have used $\Delta\eta = 0.10$ and $\Delta t^* = 0.001$ in the time interval $0 \leqslant t^* \leqslant 0.4$ and $\Delta t^* = 0.01$ for $t^* > 0.4$. A value of 20 for η_∞ was used as all solutions, for any given time t^*, converged to steady values at $\eta > 6$. It was checked that the solutions settled to their steady state profile fairly quickly (around $t^* = 0.6$) and all the runs were therefore only taken up to $t^* = 1.0$.

As this is a transient problem activated by the sudden change in the wall temperature at $t^* > 0$, both initial values of $\Delta\eta$ and Δt^* affect the value of the gradients $G'(0, t^*)$ in the early steps, as would be expected. This initial step dependency will always be present due to the sudden variation in G at $t^* > 0$, no matter how small $\Delta\eta$ or Δt^* are taken. However, provided that these initial steps are adequate (i.e. $\Delta\eta \leqslant 0.1$ and $\Delta t^* \leqslant 0.005$), the development in both directions η and t^* of the profile for $G'(\eta, t^*)$ is faithfully captured.

Results are presented for values of $t^* = 0$, 0.001, 0.01, 0.1, 0.6 and 1, in order to display the various stages in the temporal development of the solution from its successive changes in the early stages to its settlement to a new steady state. Since most shapes of practical interest lie between sphere ($c = 1$) and cylinder ($c = 0$), we have taken $0 \leqslant c \leqslant 1$.

In order to test the accuracy of our method, we have compared our surface skin friction and heat transfer results (F'_w, cS'_w, $-G'_w$) for $t^* = 0$ with those of Poots [4] and of Banks [8] and found them in excellent agreement. This comparison is shown in Fig. 2.

The temperature profile $G(\eta, t^*)$ and its negative gradient $-G'(\eta, t^*)$ for $\varepsilon = -0.1$ (i.e., the wall temperature is suddenly decreased at $t^* > 0$) and for $\varepsilon = 0.1$ (i.e., the wall temperature is suddenly increased at $t > 0$) are presented in Figs 3(a) and (b); 4(a) and (b), respectively. For $\varepsilon = -0.1$, the temperature of the fluid near the wall is found to be higher than that of the wall in a small interval of time t^* ($0 < t^* < 0.01$), because at $t^* > 0$ the wall temperature is suddenly lowered below the surrounding fluid near the wall. Also, the temperature profile $G(\eta, t^*)$ has a point of inflexion as is evident from the maximum in $-G'(\eta, t^*)$. On the other hand, for $\varepsilon = 0.1$, $G(\eta, t^*)$ monotonically decreases as η increases and there is no point of inflexion in the $G(\eta, t^*)$ profile.

The variation of the surface heat transfer parameter ($-G'_w$) with time t^* in the range $0 \leqslant t^* \leqslant 1$ for $\varepsilon = \pm 0.1$ is displayed in Figs 5 and 6. Since large changes occur in

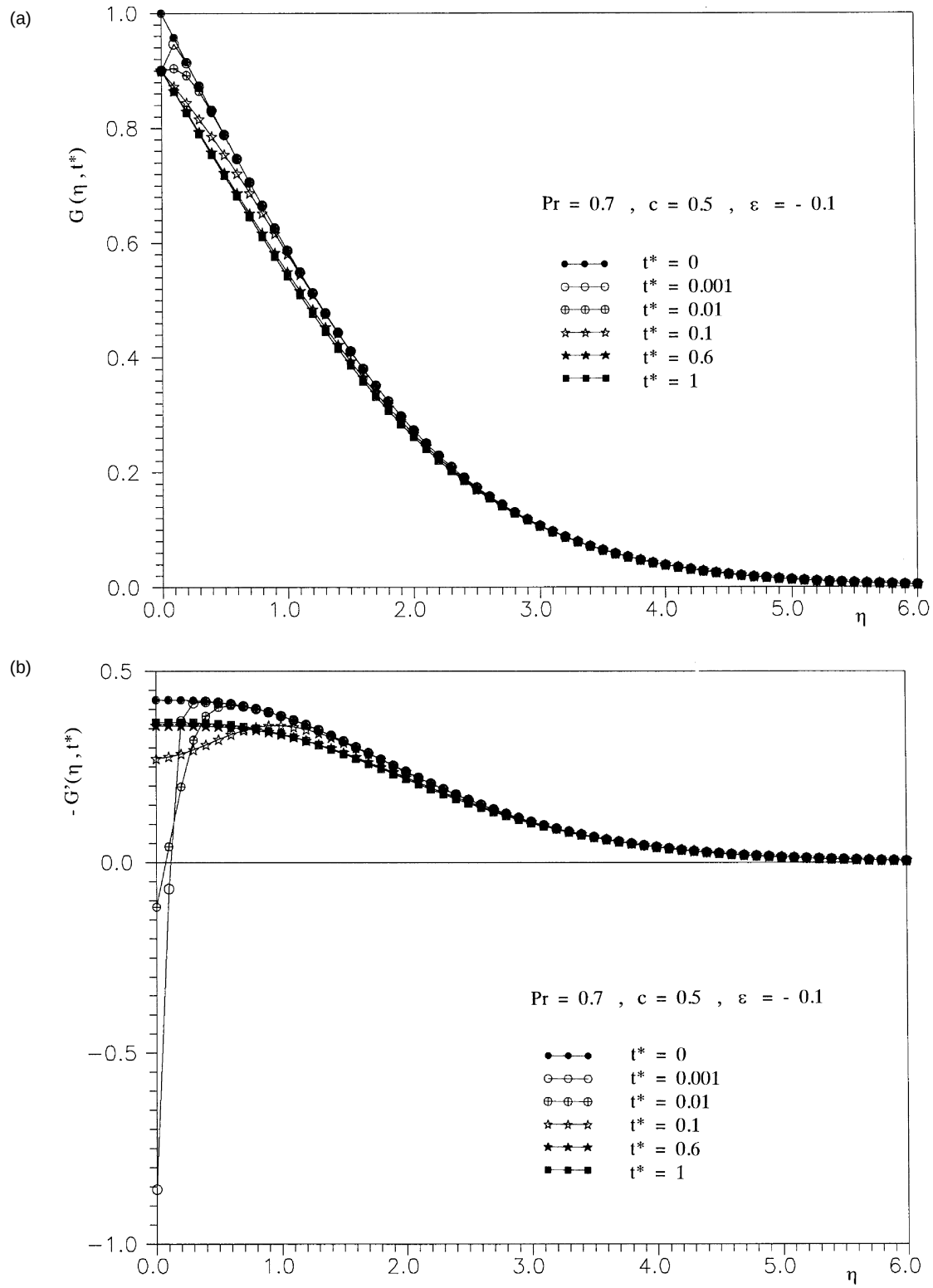

Fig. 3. (a) Temperature profiles $G(\eta, t^*)$ for various times t^*. $Pr = 0.7$; $c = 0.5$; $\varepsilon = -0.1$. (b) Temperature gradient profiles $G'(\eta, t^*)$ for various times t^*. $Pr = 0.7$; $c = 0.5$; $\varepsilon = -0.1$

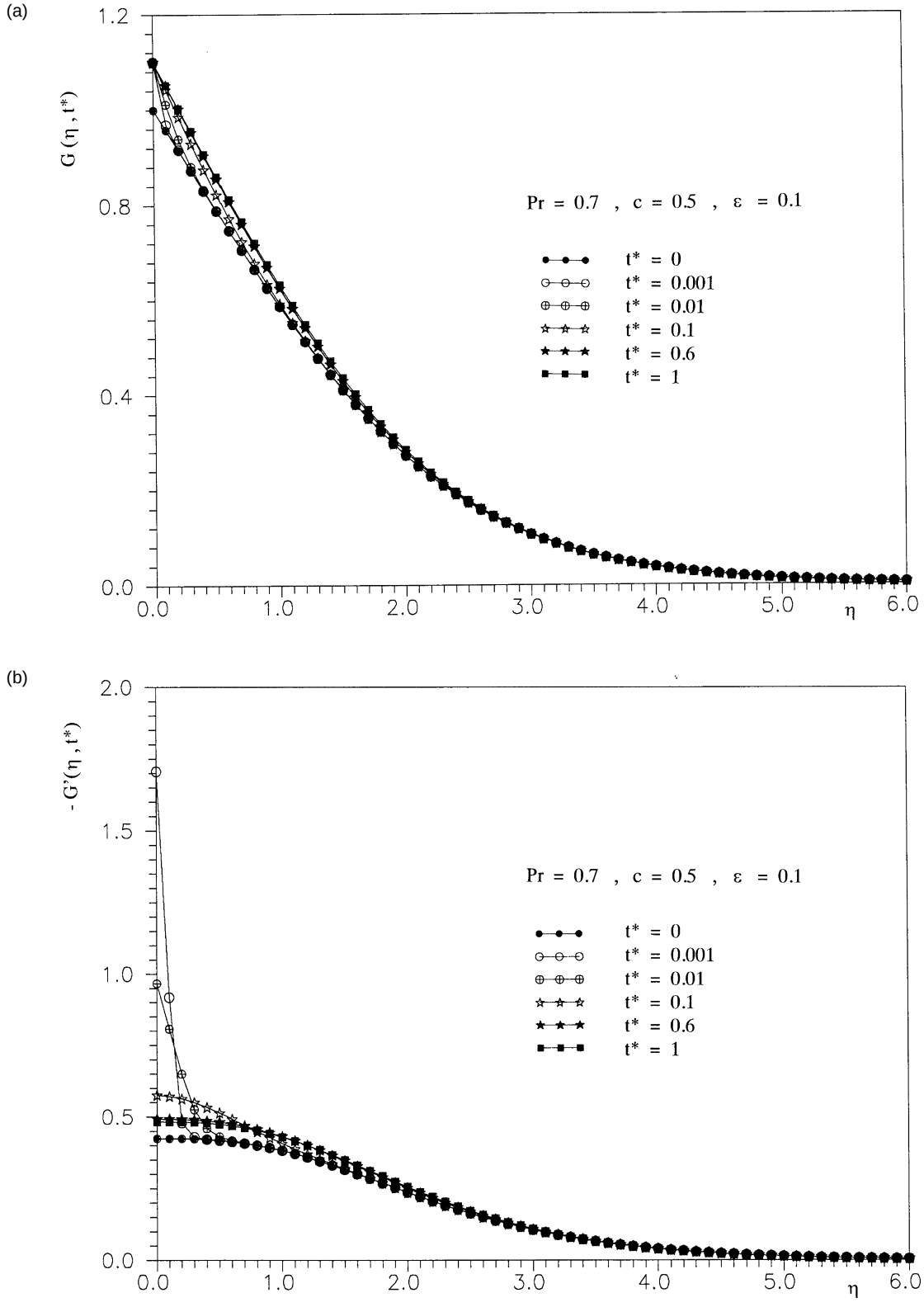

Fig. 4. (a) Temperature profiles $G(\eta, t^*)$ for various times t^*. $Pr = 0.7$; $c = 0.5$; $\varepsilon = 0.1$. (b) Temperature gradient profiles $G'(\eta, t^*)$ for various times t^*. $Pr = 0.7$; $c = 0.5$; $\varepsilon = 0.1$

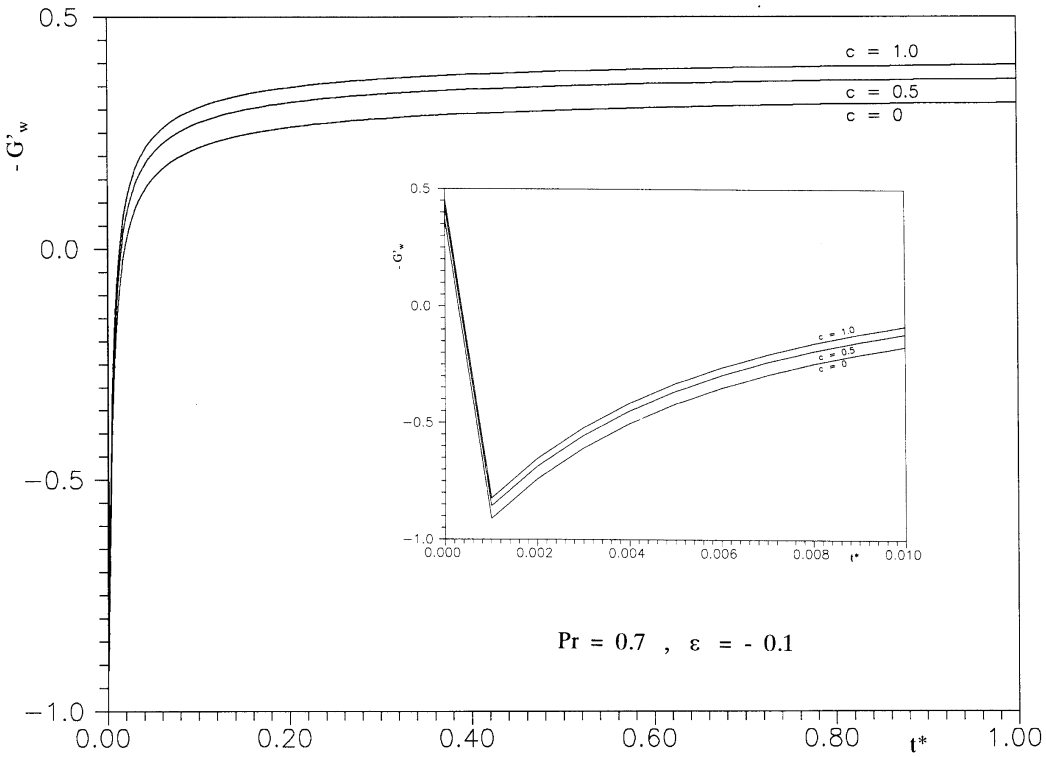

Fig. 5. Variation of the heat transfer parameter at the wall ($-G'_w$) with time t^*. $Pr = 0.7$; $c = 0, 0.5, 1$; $\varepsilon = -0.1$

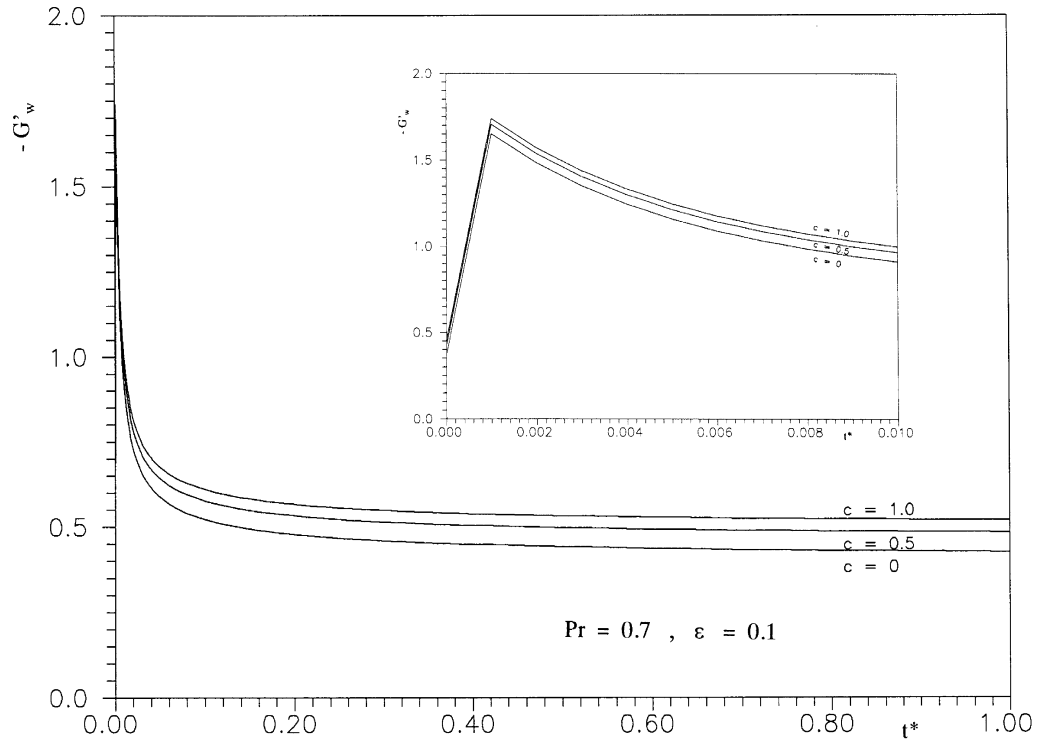

Fig. 6. Variation of the heat transfer parameter at the wall ($-G'_w$) with time t^*. $Pr = 0.7$; $c = 0, 0.5, 1$; $\varepsilon = 0.1$

a small interval of time due to the step change in the wall temperature at $t^* > 0$, the variation of $(-G'_w)$ with t^* in the interval $(0 \leqslant t^* \leqslant 0.01)$ is also given in the inset. It is observed that for $\varepsilon = -0.1$ $(-G'_w)$ goes negative during a small amount of time (<0.02) from an initial positive value at $t^* = 0$. The reason for this behaviour is that at $t^* = 0$, the wall is at a higher temperature than the surrounding fluid. Hence the heat is transferred from the wall to the fluid $(-G'_w > 0)$. At $t^* > 0$, the temperature of the wall is suddenly lowered below that of the surrounding fluid. Hence, during a small interval of time, the fluid near the wall is at a higher temperature than that of the wall. Therefore, heat transfer takes place from the fluid to the wall (i.e. $-G'_w < 0$). For $\varepsilon = 0.1$ and $t^* \geqslant 0$ the heat is transferred from the wall to the fluid (i.e., $-G'_w$ remains positive). The new steady state is reached at $t^* \sim 1$ and its value is slightly higher (for $\varepsilon = 0.1$) or slightly less (for $\varepsilon = -0.1$) than that of the initial steady state.

The variation of the surface skin friction parameters (F'_w, S'_w) with time t^* in the interval $(0 \leqslant t^* \leqslant 1)$ for $\varepsilon = \pm 0.1$ is presented in Figs 7 and 8. It is found that F'_w and S'_w change relatively little with time because the step change in wall temperature only affects F'_w and S'_w indirectly, and the values of F'_w and S'_w are slightly higher or lower than the initial steady state values depending on ε being positive or negative, respectively.

The effect of the Prandtl number Pr on the surface heat transfer parameter $(-G'_w)$ and the surface skin friction parameters (F'_w, S'_w) for $\varepsilon = 0.1$ is shown in Figs 9 and 10. Since a large change in $(-G'_w)$ takes place in a small interval of time, the inset of Fig. 9 shows the variation of $(-G'_w)$ with t^* in the interval $(0 \leqslant t^* \leqslant 0.01)$. The surface heat transfer $(-G'_w)$ increases with Pr, but the surface skin friction parameters (F'_w, S'_w) both decrease with Pr. The physical reason for this trend is that a higher Prandtl number fluid has a thinner thermal boundary layer which increases the gradient of the temperature. Consequently, the surface heat transfer is increased as Pr increases. On the other hand, the surface skin friction parameters (F'_w, S'_w) decrease as Pr increases because a higher Pr implies more viscous fluid having a comparatively larger momentum boundary layer thickness.

5. Conclusions

The results indicate that significant changes occur in the temperature and surface heat transfer in a small inter-

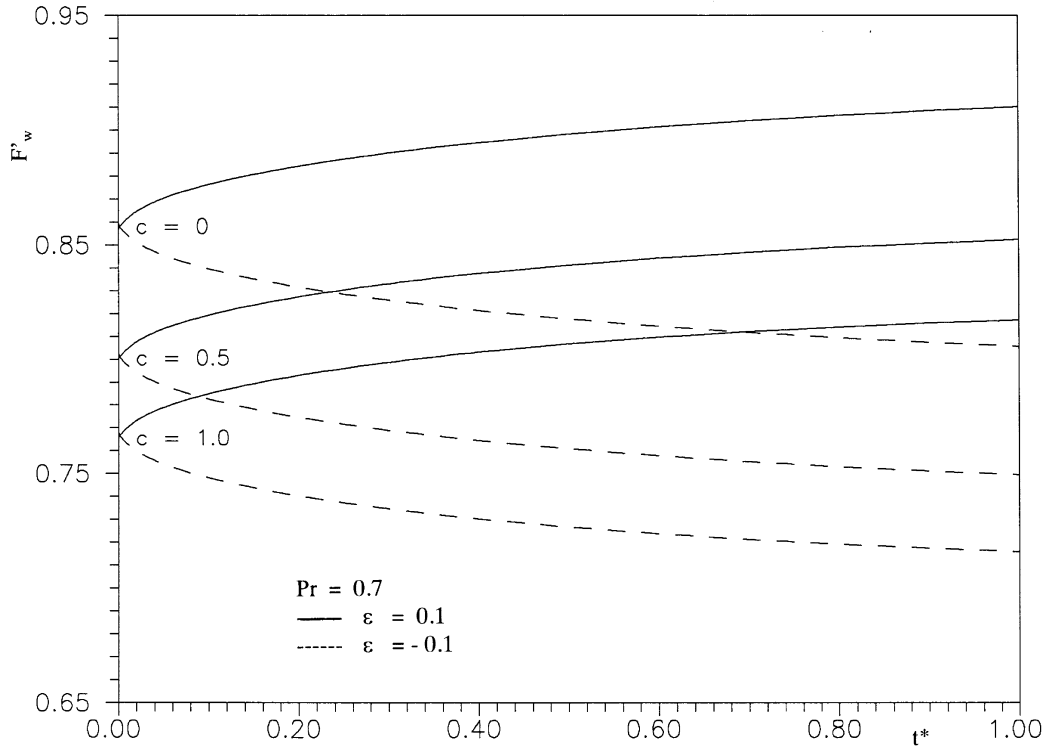

Fig. 7. Variation of the surface skin friction parameter in the x direction (F'_w) with time t^*. $Pr = 0.7$; $c = 0, 0.5, 1$; $\varepsilon = \pm 0.1$

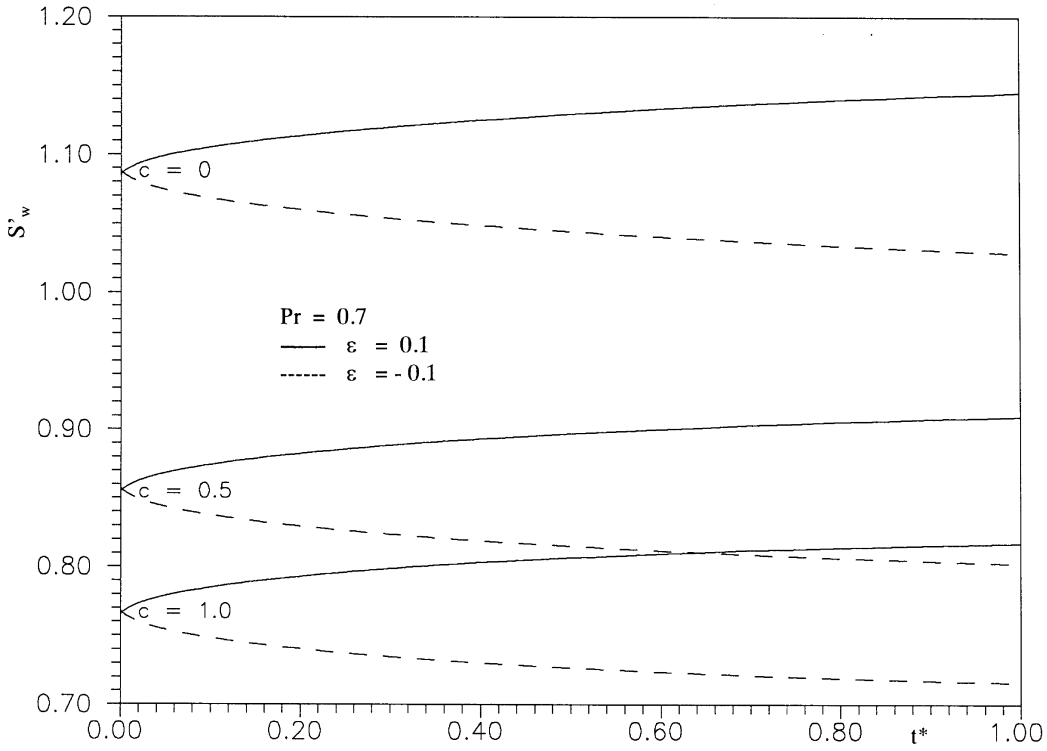

Fig. 8. Variation of the surface skin friction parameter in the y direction (S'_w) with time t^*. $Pr = 0.7$; $c = 0, 0.5, 1$; $\varepsilon = \pm 0.1$

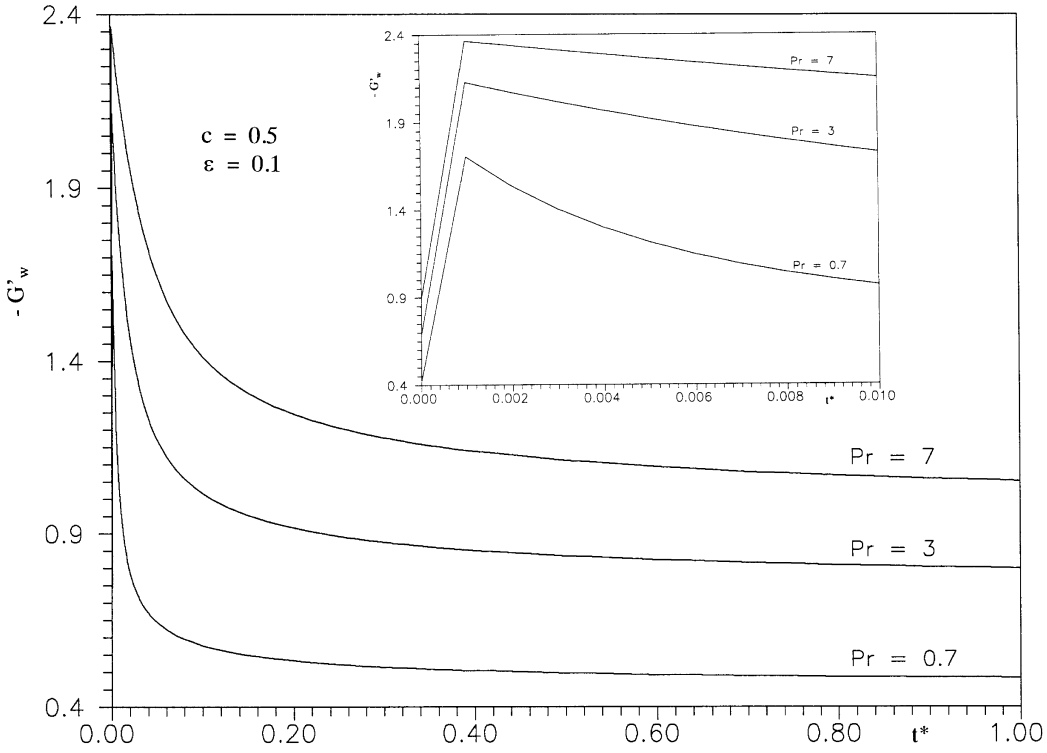

Fig. 9. Variation of the heat transfer parameter at the wall ($-G'_w$) with time t^*. $Pr = 0.7, 3.0, 7.0$; $c = 0.5$; $\varepsilon = 0.1$

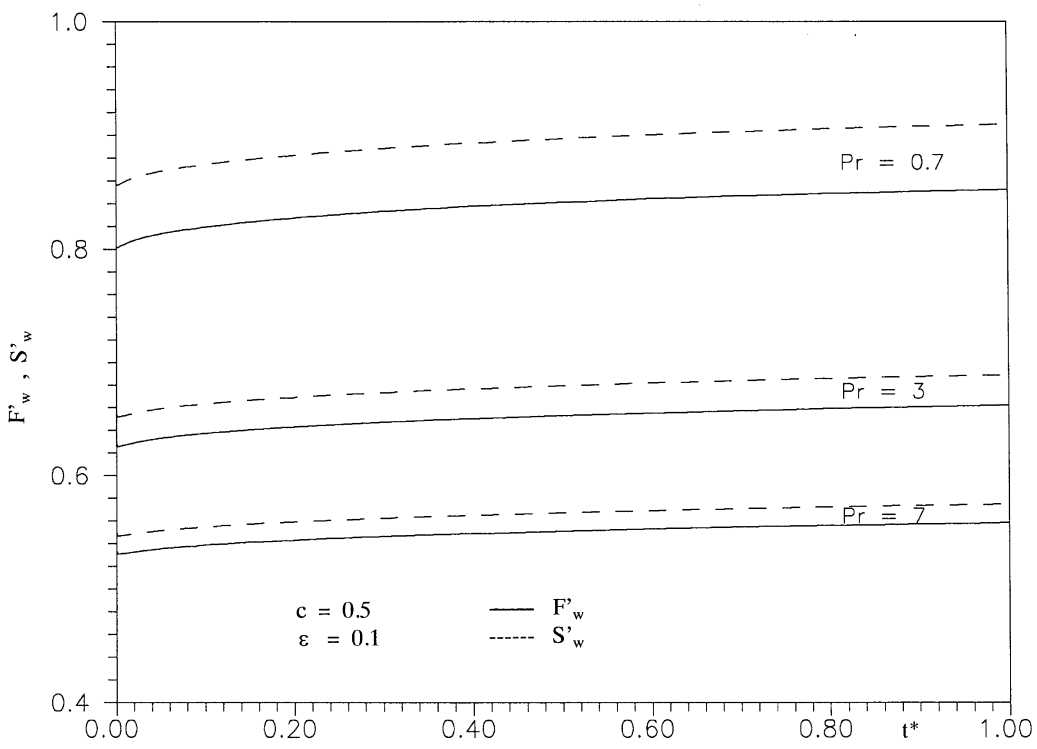

Fig. 10. Variation of the surface skin friction parameters in the x and y directions (F'_w, S'_w) with time t^*. $Pr = 0.7, 3.0, 7.0$; $c = 0.5$; $\varepsilon = 0.1$

val of time due to a step change in the wall temperature, but the skin friction parameters are relatively less affected. The new steady state is reached at time $t^* \sim 1$. When the wall temperature is suddenly reduced at $t^* > 0$, the direction of heat transfer changes during a small interval of time and the temperature profile has a point of inflexion. The surface heat transfer parameter increases with Prandtl number, while the surface skin friction parameters decrease as Prandtl number increases.

References

[1] Ede AJ. Advances in free convection. Advances in Heat Transfer 1967;4:1–64.
[2] Gebhart B. Natural convection flow and stability. Advances in Heat Transfer 1973;9:273–348.
[3] Gebhart B, Jaluria Y, Mahajan RL, Sammaria R. Buoyancy Induced Flows and Transport. New York: Hemisphere, 1988.
[4] Poots G. Laminar free convection near the lower stagnation point on an isothermal curved surface. International Journal of Heat and Mass Transfer 1964;7:863–74.
[5] Aziz K, Hellums JD. Numerical solution of the three dimensional equations of motion for laminar natural convection. Physics of Fluids 1967;10:315–24.
[6] Savage SA. Free convection flows about inclined cylinders. AIAA Journal 1969;7:1628–30.
[7] Banks WHH. Three-dimensional free convection near a two-dimensional isothermal surface. Journal of Engineering Mathematics 1972;6:109–15.
[8] Banks WHH. Laminar free convection flow at a stagnation point of attachment on an isothermal surface. Journal of Engineering Mathematics 1974;8:45–65.
[9] Ocsthuizen PH. Numerical study of some three-dimensional laminar free convection flows. Journal of Heat Transfer 1976;100:570–5.
[10] Suwono A. Laminar free convection boundary layer in three-dimensional system. International Journal of Heat and Mass Transfer 1980;23:53–61.
[11] Wilks G, Hunt R. A finite time singularity of the boundary layer equations of natural convection. ZAMP 1985;35:905–11.
[12] Childress S, Ierly GR, Spiegel EA, Young WR. Blow up of unsteady two-dimensional Euler and Navier–Stokes solutions having stagnation point form. Journal of Fluid Mechanics 1989;201:1–22.
[13] Hellums JD, Churchill SW. Transient and steady state free and natural convection: numerical solutions. AIChE Journal 1962;8:690–5.

[14] Goldstein RJ, Briggs DG. Transient free convection about vertical plates and circular cylinders. Journal of Heat Transfer 1964;86:490–500.
[15] Nanbu K. Limit of pure conduction for unsteady free convection on a vertical plate. International Journal of Heat and Mass Transfer 1971;14:1531–4.
[16] Elliot L. Free convection on a two-dimensional or axisymmetric body. Quarterly Journal of Mechanics and Applied Mathematics 1970;23:153–62.
[17] Miyamoto M. Influence of variable properties upon transient and steady-state free convection. International Journal of Heat and Mass Transfer 1977;20:1258–61.
[18] Carey VP. Analysis of transient natural convection flow at high Prandtl number using a matched asymptotic expansion technique. International Journal of Heat and Mass Transfer 1983;26:911–9.
[19] Soundalgekar VM, Ganesan P. Transient free convection with mass transfer on a vertical plate with constant heat flux. International Journal of Energy Resources 1985;9:1–18.
[20] Williams JC, Mulligan JC, Rhyne TB. Semi-similar solutions for unsteady free-convection boundary layer flow on a vertical flat plate. Journal of Fluid Mechanics 1987;175:309–32.
[21] Singh BK, Soundalgekar VM. Transient free convection of cold water past an infinite vertical porous plate. International Journal of Energy Resources 1990;14:413–20.
[22] Sattar MA, Alam MM. Thermal diffusion as well as transpiration effects on MHD free convection and mass transfer flow past an accelerated vertical porous plate. Indian Journal of Pure and Applied Mathematics 1994;25:679–88.
[23] Li BQ. The effect of magnetic fields on low-frequency oscillating natural convection. International Journal of Engineering Sciences 1996;34:1369–84.
[24] Kumari M, Slaouti A, Takhar HS, Nakamura S, Nath G. Unsteady free convection flow over a continuous moving vertical surface. Acta Mechanica 1996;116:75–82.
[25] Kumari M, Nath G. Unsteady free convection boundary layer flow at a three-dimensional stagnation point. Engineering Transactions 1984;32:3–12.
[26] Nakamura S. Iterative finite-difference schemes for similar and nonsimilar boundary layer equations. Advances in Engineering Software 1994;21:123–31.
[27] Chen TS, Yuh CF. Combined heat and mass transfer in natural convection on inclined surfaces. Numerical Heat Transfer 1979;2:233–50.
[28] Takhar HS. Free convection flow over a flat plate. Journal of Fluid Mechanics 1968;34:81–9.